

Supporting Information

Albumin/sulfonamides stabilized iron porphyrin metal organic frameworks nanocomposites: targeting tumor hypoxia by carbonic anhydrase IX inhibitor, and T₁-T₂ dual mode MRI guided photodynamic/photothermal therapy[†]

Wei Zhu,^{‡a} Yao Liu,^{‡b,c} Zhe Yang,^a Li Zhang,^a Liji Xiao,^a Pei Liu,^a Wang Jing,^a Changfeng Yi,^a Zushun Xu^{*a} and
Jinghua Ren^{*b}

^a. Hubei Collaborative Innovation Center for Advanced Organic Chemical Materials; Ministry of Education Key Laboratory for the Green Preparation and Application of Functional Materials, Hubei University, Wuhan, Hubei 430062, China.

^b. Cancer Center, Union Hospital, Tongji Medical College of Huazhong University of Science and Technology, Wuhan, Hubei 430030, China.

^c. The First Affiliated Hospital, Gannan Medical University, Ganzhou, Jiangxi, 341000, China.

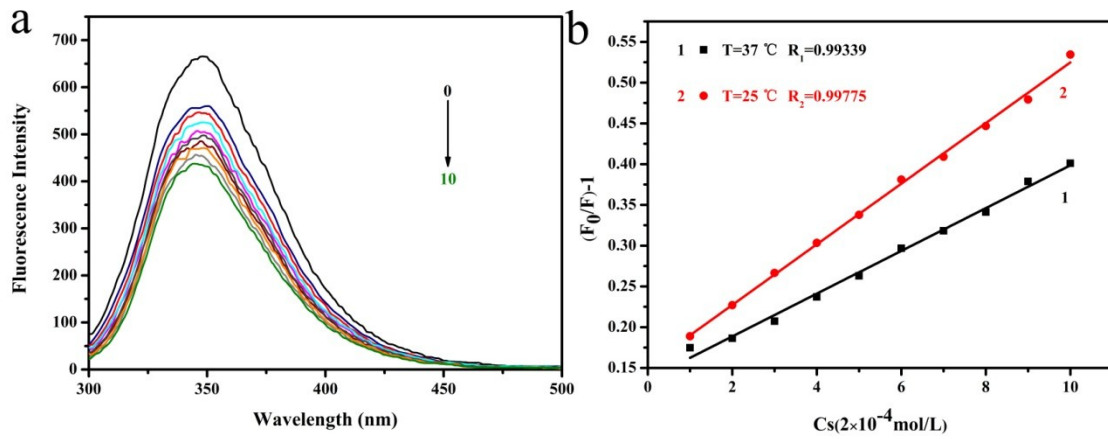


Figure S1. Fluorescence quenching study of bovine serum albumin (BSA) and sulfonamides (SAs) in H₂O solution. (a) Fluorescence spectra of BSA in the presence of SAs. (b) Stern-Volmer plots for the interaction of BSA with SAs at different temperatures.

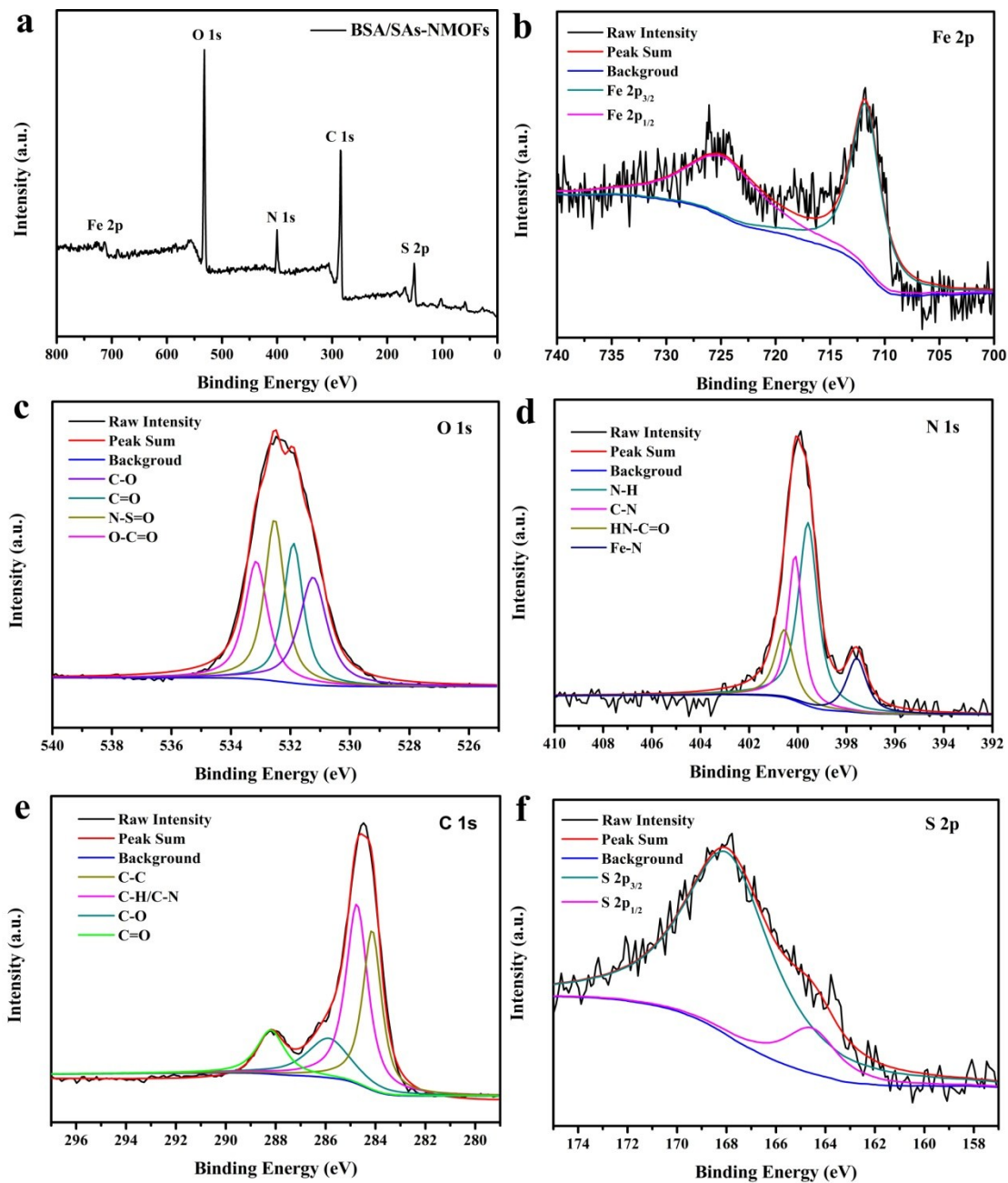


Figure S2. (a) XPS spectrum of BSA/SAs-NMOFs nanocomposites. (b), (c), (d), (e) and (f) XPS de-convoluted spectra for the Fe 2p, O 1s, N 1s, C 1s and S 2p orbitals of BSA/SAs-NMOFs nanocomposites, respectively.

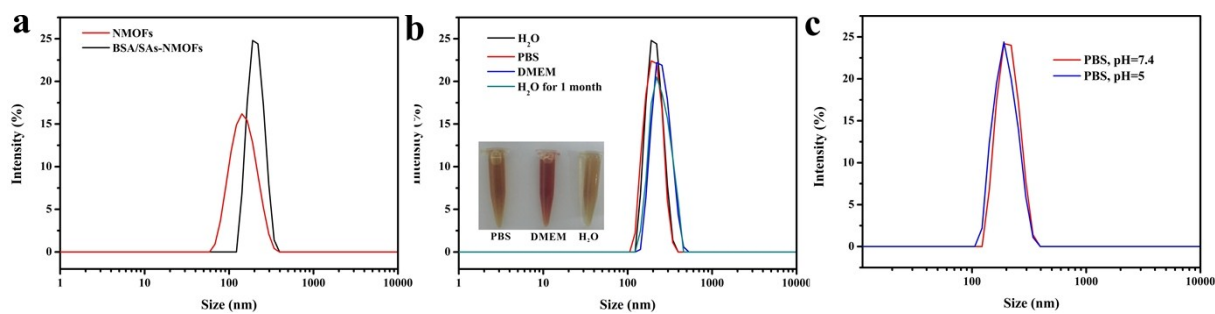


Figure S3. (a) Size distribution of NMOFs and BSA/SAs-NMOFs nanocomposites. (b) Size distribution of BSA/SAs-NMOFs nanocomposites in H₂O, PBS and DMEM. (c) Size distribution of BSA/SAs-NMOFs nanocomposites in PBS with different pH.

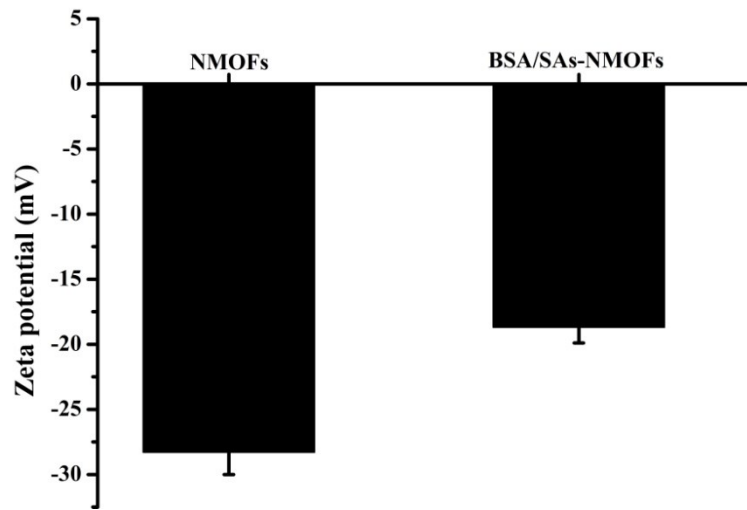


Figure S4. Zeta potentials of NMOFs NPs, and BSA/SAs-NMOFs nanocomposites dispersed in water.

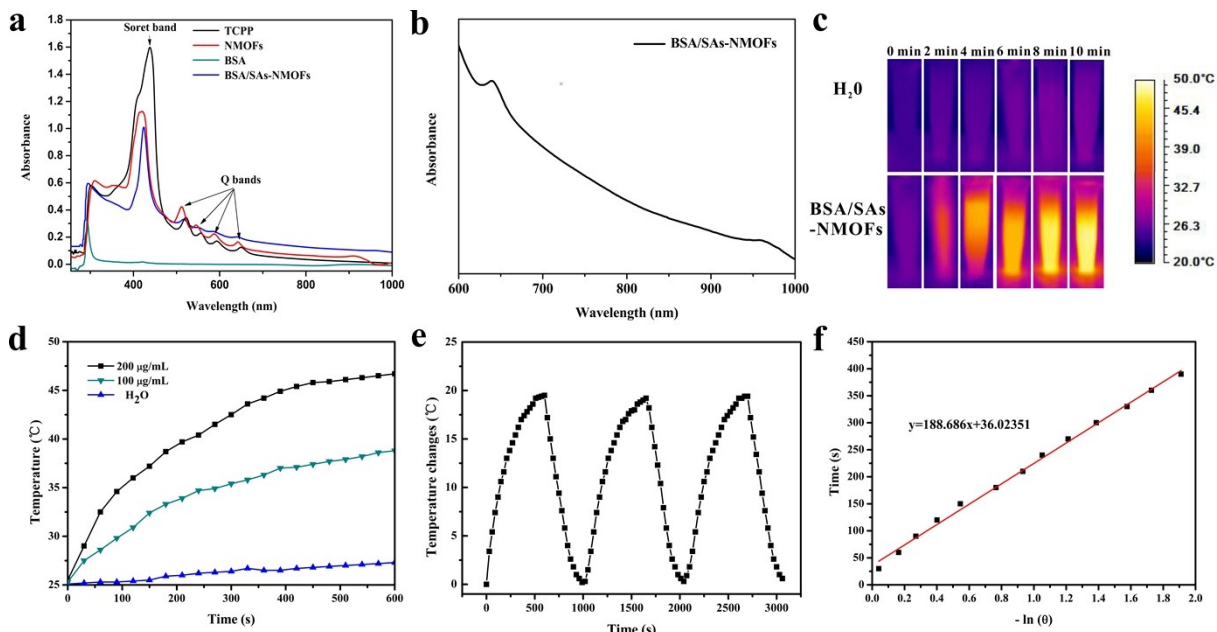


Figure S5. (a) UV-vis absorption spectra of the TCPP, NMOFs, BSA and BSA/SAs-NMOFs, they were all dilute solution of distilled H₂O. (b) Biological window absorption spectrum of BSA/SAs-NMOFs nanocomposites (200 μg/mL in distilled H₂O). (c) Infrared thermographic images of BSA/SAs-NMOFs nanocomposites (200 μg/mL in H₂O) and pure H₂O under 660 nm laser (1.0 W/cm²). (d) Temperature curves of pure water and aqueous dispersions of BSA/SAs-NMOFs nanocomposites under 660 nm laser irradiation at a power density of 1 W/cm². (e) Temperature changes of BSA/SAs-NMOFs nanocomposites during the continuous three time's laser irradiation. (f) Linear time data versus $-\ln(\theta)$ obtained from the cooling period.

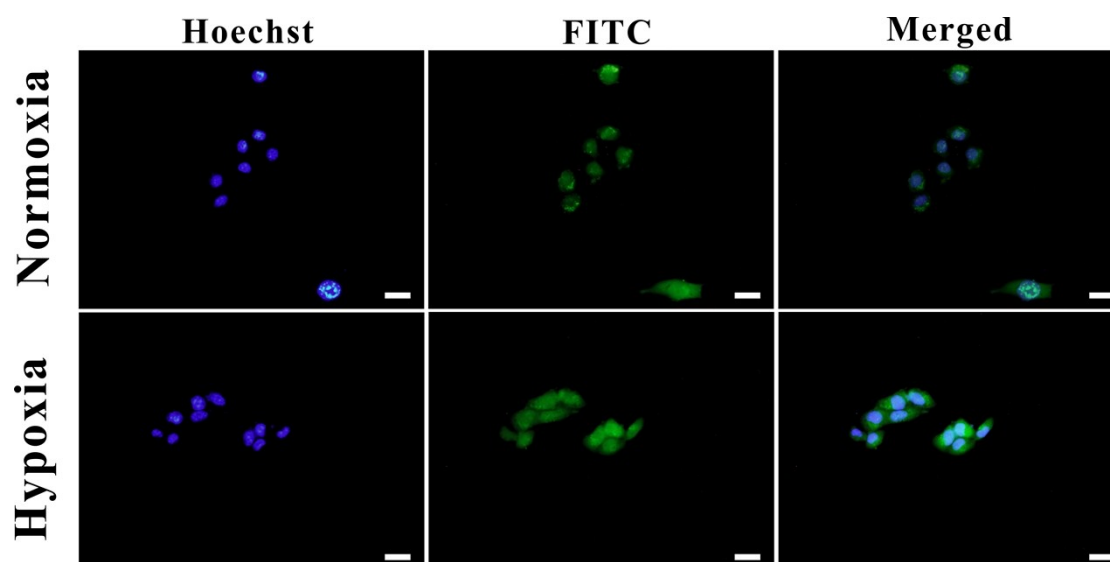


Figure S6. Fluorescence images of 4T1 cells incubated with 200 $\mu\text{g}/\text{mL}$ of BSA/SAs-NMOFs labeled FITC nanocomposites after 4 h under normoxia (21% O_2) and hypoxia (1% O_2), respectively. And its blue and green emission in Hoechst 33342 ($\lambda_{\text{ex}} = 350 \text{ nm}$, $\lambda_{\text{em}} = 460 \text{ nm}$) and FITC ($\lambda_{\text{ex}} = 488 \text{ nm}$, $\lambda_{\text{em}} = 520 \text{ nm}$) channels.

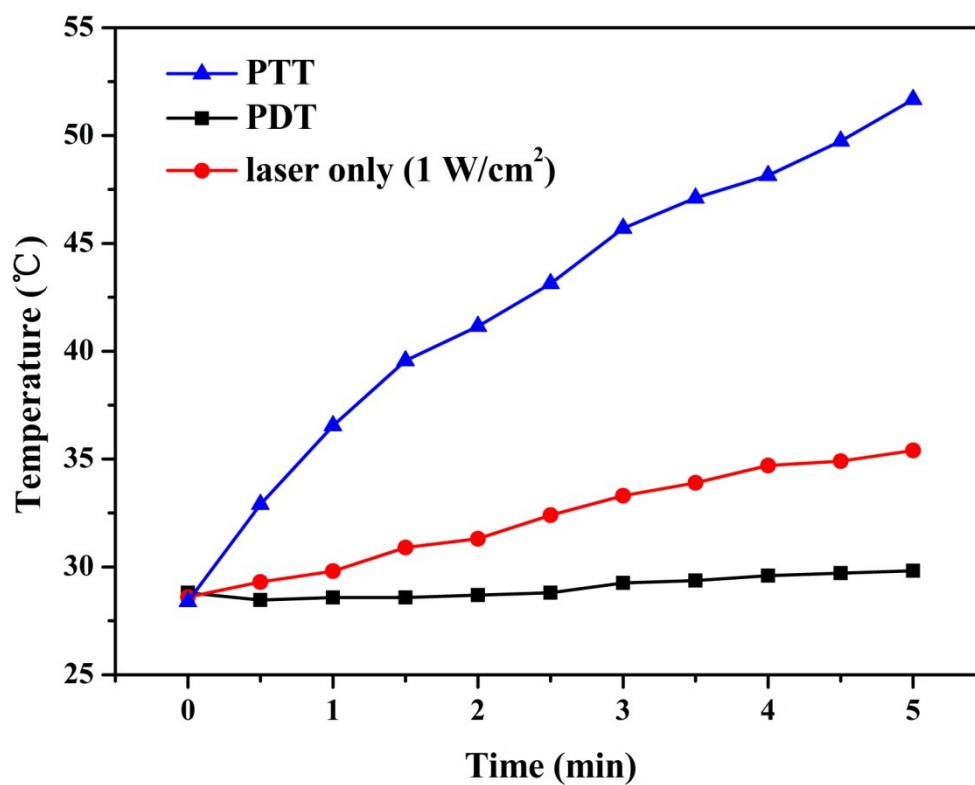


Figure S7. Temperature curves of tumor site treated with BSA/SAs-NMOFs nanocomposites (10 mg/kg per mouse) under 660 nm laser irradiation at a power density of 1 W/cm², 660 nm (50 mW/cm²) and laser only (660 nm 1 W/cm²), respectively.

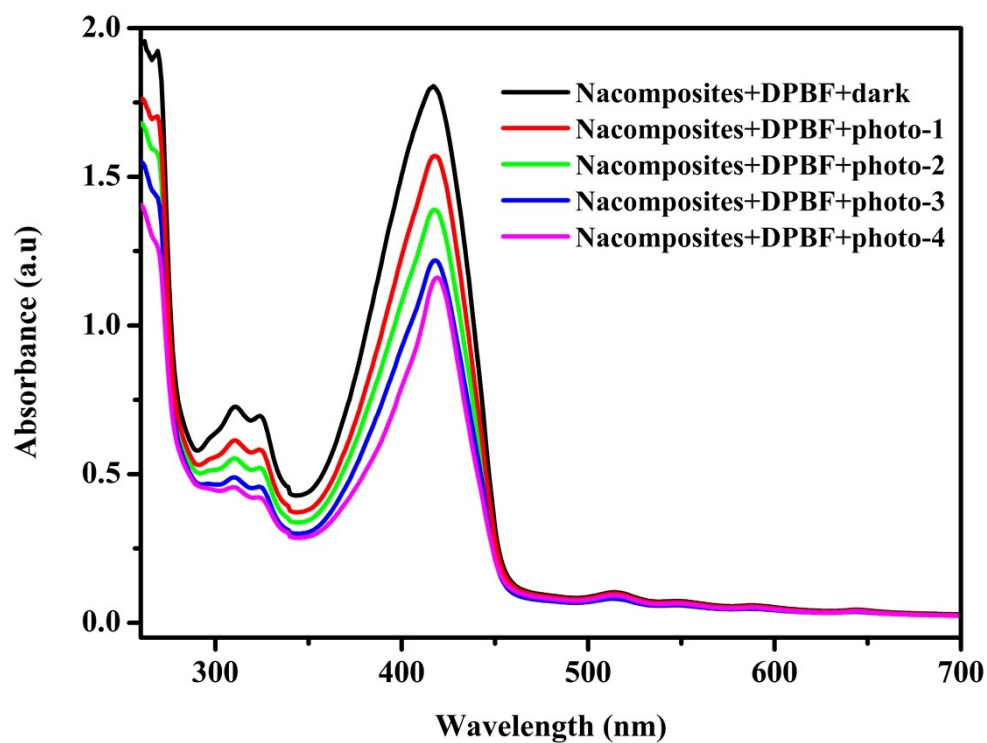


Figure S8. The UV-Vis-NIR absorption spectra of DPBF (0.05 mM, ethanol) recorded after various treatment in the presence of BSA/SAs-NMOFs nanocomposites under dark and photo irradiation conditions. Photo-1: 50 mW/cm² for 10 min; Photo-2: 1 W/cm² for 5 min; Photo-3: 50 mW/cm² for 10 min, then 1 W/cm² for 5 min; Photo-4: 1 W/cm² for 5 min, then 50 mW/cm² for 10 min. The all BSA/SAs-NMOFs nanocomposites were dispersed in deionized water (200 µg/mL)

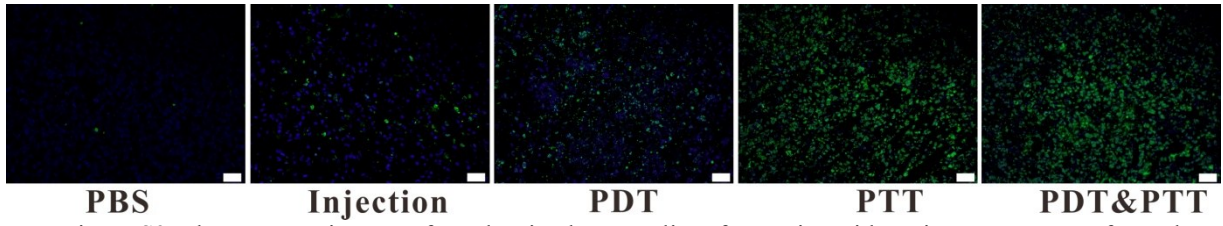


Figure S9. Fluorescence images of tunel stained tumor slices from mice with various treatments after 7 days.